Hypoxia-Regulated Delta-like 1 Homologue Enhances Cancer Cell Stemness and Tumorigenicity

Yuri Kim,[1] Qun Lin,[1] Daniel Zelterman,[2] and Zhong Yun[1]

Departments of [1]Therapeutic Radiology and [2]Epidemiology and Public Health, Yale University School of Medicine, New Haven, Connecticut

Abstract

Reduced oxygenation, or hypoxia, inhibits differentiation and facilitates stem cell maintenance. Hypoxia commonly occurs in solid tumors and promotes malignant progression. Hypoxic tumors are aggressive and exhibit stem cell–like characteristics. It remains unclear, however, whether and how hypoxia regulates cancer cell differentiation and maintains cancer cell stemness. Here, we show that hypoxia increases the expression of the stem cell gene *DLK1*, or *delta-like 1 homologue* (*Drosophila*), in neuronal tumor cells. Inhibition of *DLK1* enhances spontaneous differentiation, decreases clonogenicity, and reduces *in vivo* tumor growth. Overexpression of *DLK1* inhibits differentiation and enhances tumorigenic potentials. We further show that the DLK1 cytoplasmic domain, especially Tyrosine339 and Serine355, is required for maintaining both clonogenicity and tumorigenicity. Because elevated *DLK1* expression is found in many tumor types, our observations suggest that hypoxia and *DLK1* may constitute an important stem cell pathway for the regulation of cancer stem cell–like functionality and tumorigenicity. [Cancer Res 2009;69(24):9271–80]

Introduction

How a tumor is initiated, sustains its growth, and progresses toward malignancy remains an ardently pursued topic. The cancer stem cell model posits that tumor growth is sustained by a small population of cancer cells that, like normal stem cells, are capable of self-renewal and differentiation (1). In contrast, the stochastic or clonal evolution model states that most of the tumor cells within a growing tumor mass are capable of self-renewal and that heterogeneity results from interclonal variations (2). For the most part, the majority of tumors, especially solid tumors, may be more appropriately explained by a combination of these two prevailing models (2). In either case, the tumor microenvironment may have profound impact on how cancer stem cells are maintained or how subclones with growth and survival advantages evolve and are selected. Currently, little is known about the role of the tumor microenvironment on the maintenance of stem cell characteristics, the cell-fate decision, and tumorigenic potential of poorly differentiated cancer cells.

Solid tumors contain regions with oxygen deficiency or hypoxia, and tumor hypoxia predicts poor clinical outcomes (3). Hypoxic tumor cells appear to be highly tumorigenic and poorly differentiated with expression of stem cell markers (4, 5). Expression of hypoxia-inducible factor (HIF)-1α is elevated in poorly differentiated pancreatic cancers (6). HIF-2α appears to be preferentially expressed in stem cell–like populations in neuroblastoma (NB) and brain tumors (7, 8). These observations reveal a strong correlation between the hypoxia pathways and cancer stem cell characteristics. We and others have shown that hypoxia can inhibit differentiation of embryonic stem cells and progenitor cells (9–12). Interestingly, we found (11) that hypoxia arrested adipogenic progenitor cells in an undifferentiated state and increased expression of DLK1, or delta-like 1 homologue (*Drosophila*), a type I transmembrane protein preferentially expressed in embryonic tissues and immature cells (13). Elevated expression of DLK1 is also reported in several tumor types, especially neuronal tumors such as NB and glioma (14–19). However, the role of DLK1 in tumor development or progression remains to be examined. Using NB cells as a model, we show that expression of DLK1 is increased by hypoxia and plays an essential role in the maintenance of the undifferentiated NB phenotype, their clonogenic potential, and their tumorigenicity *in vivo*. This previously unknown hypoxia-regulated stem cell pathway may have the potential to regulate the maintenance of cancer stem cell characteristics and to promote tumor progression.

Materials and Methods

Cell culture and hypoxia. SK-N-BE(2)C [BE(2)C], SK-N-ER (ER), and SH-SY5Y (SY5Y) cells were maintained in MEM and F12 (1:1), and IMR32 cells, in MEM, supplemented with 10% fetal bovine serum, 1 mmol/L sodium pyruvate, and 25 mmol/L HEPES at pH 7.4. Retroviral infection was described previously (11, 12). All-*trans*-retinoic acid (RA) or bromodeoxyuridine (BrdUrd) was used to induce differentiation. Hypoxia (1% O_2) experiments were performed in a hypoxia chamber (Invivo$_2$ 400, Ruskinn Technology) and anoxia experiments were performed in a Bactron Anaerobic Chamber (Sheldon MFG, Inc.). Deferoxamine mesylate (Sigma-Aldrich) was used to mimic hypoxia effects at 21% O_2 (11, 12). Culture media were replaced every other day inside the hypoxia chamber.

Tumor sphere culture. Cells were plated at 30,000 cells/mL in the sphere medium (see Supplementary Materials and Methods for details). To facilitate sphere formation, tissue culture dishes were coated with polyhydroxyethylmethacrylate (polyHEMA; Sigma-Aldrich) as described in Supplementary Materials and Methods. Cells were dissociated by repeated pipetting or with 0.05% trypsin to obtain single-cell suspension for passages or for cell counting.

Plasmids. The retroviral DLK-FL (full-length DLK1) and DLK-ΔCyto (without the cytoplasmic domain) constructs containing the *GFP* gene were provided by Dr. R. Bhatia (City of Hope National Medical Center, Duarte, CA; ref. 19). The mutations in the DLK1 cytoplasmic domain, Y339F, S355A, and Y339F/S355A, were created using the QuikChange site-directed mutagenesis kit (Stratagene). The constitutively active HIF-1α mutant (P402G/P564A) was described previously (20). The constitutively active HIF-2α mutant

Note: Supplementary data for this article are available at Cancer Research Online (http://cancerres.aacrjournals.org/).

Requests for reprints: Zhong Yun, Department of Therapeutic Radiology, Yale University School of Medicine, P. O. Box 208040, New Haven, CT 06520-8040. Phone: 203-737-2183; Fax: 203-785-6309; E-mail: zhong.yun@yale.edu.

doi:10.1158/0008-5472.CAN-09-1605

(Pro531A) was obtained from Dr. F. Lee (University of Pennsylvania School of Medicine, Philadelphia, PA; ref. 21) and was subcloned into the pLZRS retroviral vector.

The lentiviral short hairpin RNA (shRNA) constructs (shDLK-2H and shDLK-4H) were cloned into CS-CDF-EG-PRE-K1f (22), and the siRNA oligonucleotides (siDLK-05 and siFLK-07) were from Dharmacon. Detailed cloning information and nucleotide sequences are shown in Supplementary Materials and Methods.

Real-time reverse transcription-PCR. First-strand cDNA was synthesized from total RNA. Real-time PCR was performed on StepOne Plus (Applied Biosystems) using Power SYBR Green PCR Master Mix (Applied Biosystems) according to the manufacturer's recommended protocol. The primer sequences can be found in Supplementary Materials and Methods.

Chromosome immunoprecipitation. BE(2)C cells were incubated at 1% O_2 for 16 to 18 h and were used for chromosome immunoprecipitation (ChIP) according to our previously published protocol (20). The detailed procedure and ChIP primer sequences can be found in Supplementary Materials and Methods.

Northern blot. Total RNA was fractionated in 1% agarose gel and hybridized at 65°C overnight in Church's Buffer with an [α-^{32}P] dCTP–labeled DLK1/pref-1 cDNA probe prepared from pCMV-Sport6.1-pref-1 (IMAGE 6393667). The radioactive blots were visualized on a Storm 860 PhosphorImager (GE Healthcare).

Western blot. Western blot was done as described previously (11) with the following antibodies: polyclonal rabbit anti-DLK1 (1:3,000; Chemicon International); anti-Sox2 (1:1,000; Chemicon International); c-kit (1:500; Zymed Laboratories); CD-133 (1:100; Abgent,); Notch1 (1:2,000), HIF-1α (1:2,000), and HIF-2α (1:1,000; Novus Biologicals); proliferating cell nuclear antigen (PCNA; 1:500; Santa Cruz Biotechnology); and phospho–extracellular signal-regulated kinase (ERK) and total ERK (1:1,000; Cell Signaling), or β-actin (1:20,000; Sigma-Aldrich).

Cell proliferation assay (MTS). BE(2)C cells were transduced with lentivirus for 48 h and then reseeded at a density of 2×10^4 cells per well in 96-well plates. Cell growth was then analyzed every day using the MTS assay (Promega).

Immunofluorescence. Cells were fixed for 10 min with –20°C methanol and then incubated with mouse anti-DLK1 (1:100; R&D Systems) or rabbit anti–β-tubulin III (1:100; Sigma-Aldrich), followed by incubation with Alexa 594–conguated donkey-anti-mouse (1:500; Invitrogen) or Alexa 488–conguated goat-anti-rabbit (1:500; Invitrogen). Hoechst 33342 (2 μg/mL) was used for nuclear staining.

Clonogenic assays. NB cells were plated at 300 to 500 cells per well in six-well plates for 10 to 14 d, and colonies were stained with crystal violet. Plating efficiency = number of colonies (≥50 cells per colony) per input cells × 100%.

Tumor xenografts. NB cells were harvested by trypsinization, resuspended in cold PBS, then mixed with an equal volume of Matrigel (BD Bioscience), and then injected (100 μL/site) s.c. on both sides of the anterior backs of a group of five *NU/J* mice (6-wk-old males; Jackson Laboratory). Tumor growth was monitored twice weekly. Tumor take was recorded when a palpable tumor was detected. Tumor size was measured using a precision caliper as the longest surface length (mm; L) and width (W). Tumor volume (V; mm^3) = $LW^2/2$ (23). All protocols were reviewed and approved by the Yale Institutional Animal Care and Use Committee.

Statistics. The statistical difference between two groups was analyzed by the two-tailed, unpaired Student's t test using Prizm 3.0 (GraphPad Software, Inc.). All results are expressed as mean ± SEM. For statistical analysis of tumor growth, the general statistical model used is:

$$\log(volume) = \alpha + \beta \log(t)$$

where α and β are constants, and t is the elapsed time. Large values of α correspond to uniformly larger tumor sizes across all dates. The slope β measures the rate of growth on this log scale. Statistical analysis was performed using linear regression in time.

Results

Hypoxia increases *DLK1* expression. DLK1 was strongly increased at both mRNA and protein levels (Supplementary Fig. S1*A* and Fig. 1*A*) either at 1% O_2 (hypoxia) or in the presence of deferoxamine, a hypoxia-mimicking compound in a panel of NB cell lines with *MYCN* amplification [BE(2)C and IMR32] or without *MYCN* amplification (ER and SY5Y). DLK1 expression can also be induced under anoxia (Supplementary Fig. S1*B*). We chose 1% O_2 because it is close to the pO_2 threshold (5–10 mmHg or 0.7–1.3% O_2) widely used in clinical studies to define tumor hypoxia *in vivo* (3). We further found that hypoxia also increased DLK1 expression in glioblastoma cells as well as normal neuronal progenitor cells (Supplementary Fig. S1*B* and *C*), suggesting a common regulatory mechanism for *DLK1* expression by hypoxia in neuronal progenitor cells and neuronal tumors. DLK1 is predominantly expressed as a full-length protein with a relative motility of around 50 kDa (Fig. 1*A, left*). An ~45 kDa form of DLK1 was found in ER cells (Fig. 1*A, lanes 5–6*), likely due to the enzymatic cleavage of its extracellular domains (24).

Hypoxia induced the expression of HIF-1α protein in all the NB cell lines (Fig. 1*A, left*). Other hypoxia-inducible genes, such as vascular endothelial growth factor (VEGF) and glucose transporter 1 (GLUT1), were also induced by hypoxia (Supplementary Fig. S2*A* and *B*). However, only BE(2)C and SY5Y cells expressed HIF-2α (Supplementary Fig. S2*C* and *D*), and the HIF-2α expression was independent of the *MYCN* status. It is likely that a combination of HIF-α expression and the *MYCN* status could potentially explain different levels of DLK1 expression in NB cells.

Importantly, HIF-1α or HIF-2α alone is sufficient to enhance DLK1 expression (Fig. 1*B, left*), whereas deletion of both HIF-1α and HIF-2α is needed to abolish hypoxia-dependent increase of DLK1 expression (Fig. 1*B, right*). The proximal 5′ promoter/enhancer region of the *DLK1* gene contains three putative hypoxia responsive elements (HREs) with the conserved motif of 5′-ACGTG-3′ (25) at –758, –402, and –248 bp, respectively. To ascertain HIF binding by ChIP assays, we designed two sets of primers flanking the HRE at –758 bp (DLK1-3D) and –248 bp (DLK1-4P), respectively. Both HIF-1α and HIF-2α were coimmunoprecipitated with this proximal *DLK1* promoter/enhancer region in hypoxia-treated cells as determined by amplicons with the predicted sizes (Fig. 1*C, left*) and by qRT-PCR (Fig. 1*C, right*). No promoter binding was found using the control IgG. Neither anti–HIF-1α nor anti–HIF-2α antibody precipitated the *RAD51* promoter, a HIF-independent gene (26), further demonstrating the specificity of HIFs toward the *DLK1* promoter. Consistent with the literature (7, 27), HIF-1α appeared to bind the *VEGFA* promoter more efficiently than HIF-2α did. These data clearly show that hypoxia increases *DLK1* transcription via the HIF-dependent mechanism.

***DLK1* facilitates the maintenance of an undifferentiated NB phenotype.** We focused on BE(2)C cells because they have a high level of DLK1 expression (Fig. 1*A*) and possess cancer stem cell characteristics (28, 29). We found that *DLK1* mRNA (Fig. 1*D, lane 3*) and protein (Fig. 1*D, lane 7*) were strongly decreased upon RA-induced differentiation. Interestingly, *DLK1* expression was maintained by hypoxia (1% O_2) even in the presence of RA (Fig. 1*D, lanes 4* and *8*). This result was consistent with the observation that hypoxia decreased RA-induced neurite growth, a hallmark of neuronal differentiation (Supplementary Fig. S3). In addition to RA, BrdUrd, an inducer of non-neuronal differentiation (28, 29), also dramatically decreased DLK1 expression as

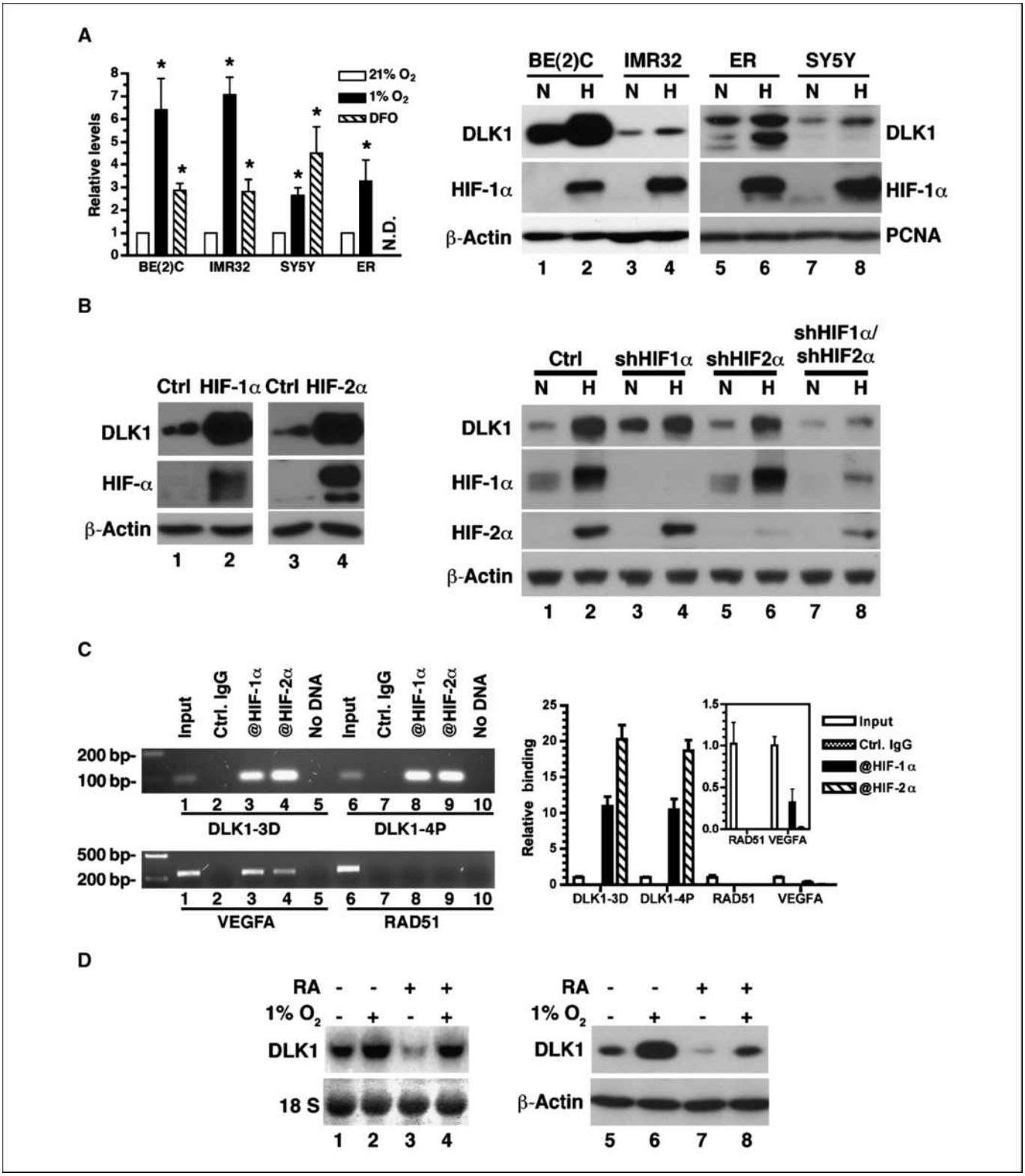

Figure 1. Hypoxia induces DLK1 expression. *A,* quantitative reverse transcription-PCR (*left*) for *DLK1* mRNA. Total RNA was prepared from NB cells after 16 h of incubation at 1%, 21% O_2, or in the presence of 100 μmol/L deferoxamine. Data were normalized to *HPRT* mRNA that did not change under hypoxia (*columns,* mean from ≥3 experiments; *bars,* SEM; *, $P < 0.05$). Western blot for DLK1 (*right*) with HIF-1α as a control for hypoxia and β-actin or PCNA as a loading control. *N.D.,* not determined. *B,* Western blot for DLK1. BE(2)C cells were transduced with retrovirus containing either the constitutively active HIF-1α, constitutively active HIF-2α, or empty vector (*ctrl*; *left*) or with lentivirus expressing shHIF1α, shHIF2α, or simultaneously infected with both shHIF1α and shHIF2α virus (*right*). Cells were cultured for 16 h at 1% (hypoxia, *H*) or 21% O_2 (*N*). *C,* ChIP using @HIF-1α or @HIF-2α antibodies. BE(2)C cells were incubated at 1% O_2 for 16 h to induce the HIF-α subunits. Two different sets of primers (DLK1-3D and DLK1-4P) were used to detect the *DLK1* promoter gene with *RAD51* primers as negative control and *VEGFA* primers as positive control. Amplicons with the predicted sizes were validated using the end-point PCR for 28 cycles (*left*). Relative levels of promoter binding were analyzed by qRT-PCR (*right*). *D,* Northern (*left*) and Western blot (*right*) for DLK1 in BE(2)C cells cultured at 1% (+) or 21% (–) O_2 with or without 1 μmol/L RA for 24 h.

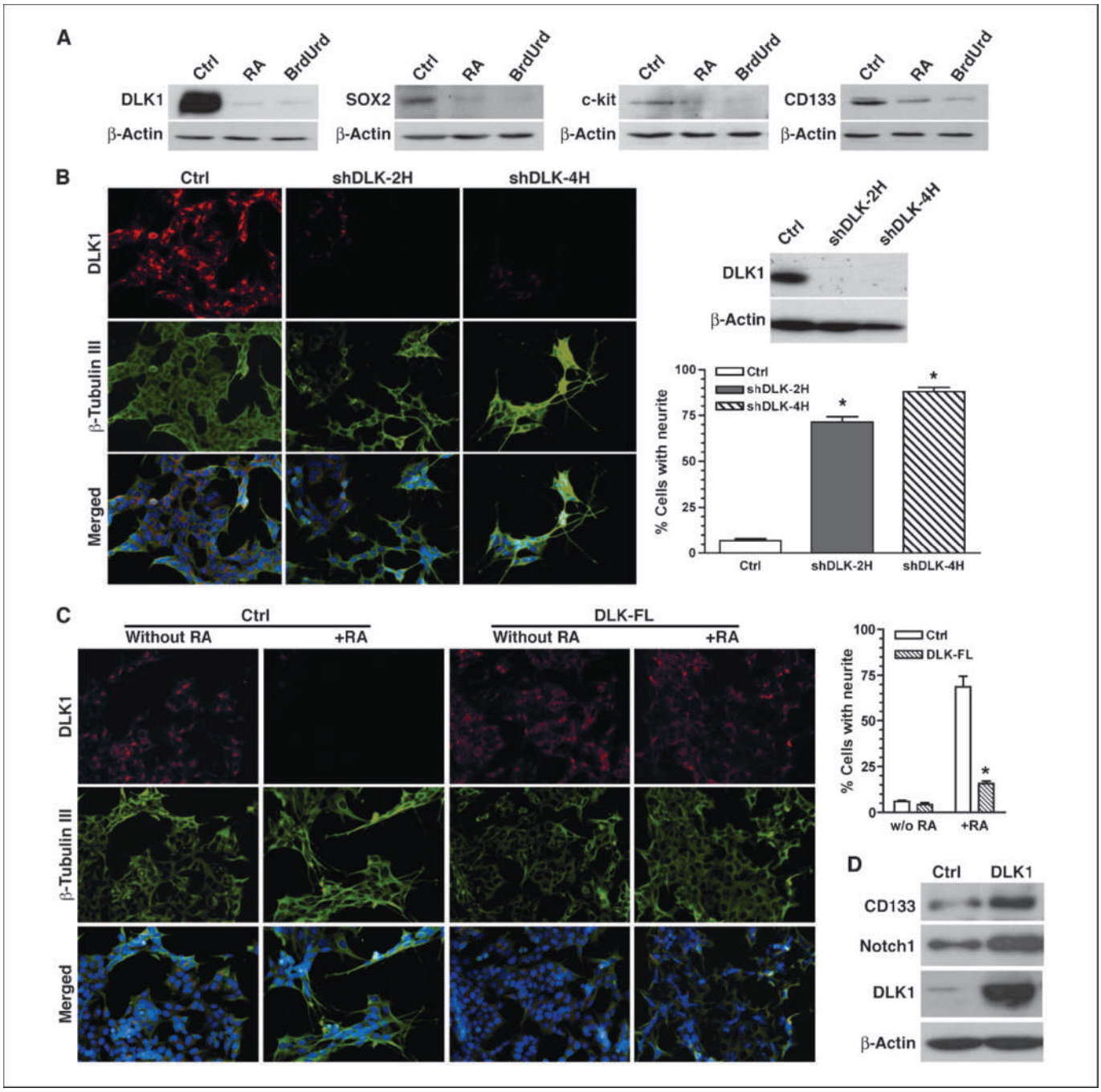

Figure 2. DLK1 maintains an undifferentiated NB phenotype. *A,* BE(2)C cells were differentiated with 1 μmol/L RA or 10 μmol/L BrdUrd for 5 d. DLK1, Sox2, c-kit, and CD-133 were detected by Western blot. *B,* BE(2)C cells were infected with lentivirus expressing shDLK-2H, shDLK-4H, or empty lentiviral vector (*ctrl*). *Left:* Infected cells were stained using antibodies against DLK1 (*red*) or neuron-specific β-tubulin III (*green*) with Hoechst 33342 as nuclear stain (*blue*). Magnification, ×200. *Right,* expression of DLK1 was analyzed by Western blot, and cells with β-tubulin III–positive neurites were enumerated from five to six random fields (*columns,* mean; *bars,* SEM; *, $P < 0.0001$ versus control). *C, left,* fluorescence-activated cell sorting (FACS)–selected BE(2)C cells expressing the full-length DLK1 (*DLK-FL*) or empty retroviral vector (*ctrl*) were cultured for 3 d with or without 1 nmol/L RA and then stained as in *B.* Magnification, ×200. *Right,* neurite-positive cells were counted from five to six random fields (*columns,* mean; *bars,* SEM; *, $P = 0.0001$ versus RA-treated control). *D,* Western blot for CD133 and Notch1 in ER cells expressing the full-length DLK1 with the empty retroviral vector as control (*ctrl*).

shown by indirect immunofluorescence (Supplementary Fig. S4*A*). We further found (Fig. 2*A*) that DLK1 expression was highly correlated with the expression of other neuronal stem cell markers including c-kit, CD-133, and SOX2 (29, 30). These observations show that DLK1 is a bona fide stem/progenitor cell marker for immature NB cells.

To examine the role of *DLK1* in NB cell differentiation, we designed two lentivirus-based shRNA interference constructs, shDLK-2H and shDLK-4H, which target two separate regions of *DLK1* mRNA. Both shDLK constructs inhibited expression of endogenous *DLK1* in BE(2)C cells (Fig. 2*B*), although shDLK-4H appeared to be more effective (up to 2-fold more efficient based

on qRT-PCR analysis) than shDLK-2H in decreasing *DLK1* mRNA. Interestingly, BE(2)C cells with *DLK1* knockdown spontaneously developed neuronal processes under normal culture conditions, as revealed by immunofluorescence of the neuron-specific β-tubulin III (Fig. 2*B*). Spontaneous differentiation was observed only in cells expressing shDLK-2H or shDLK-4H but not in control-infected cells (Supplementary Fig. S4*B*). We further confirmed this observation using two separate siRNA oligonucleotides (Supplementary Fig. S4*C*). We also found that expression of the sympathetic neuronal peptide neurotransmitter gene neuropeptide tyrosine (*NPY*; ref. 5) was increased in BE(2)C cells either treated with RA or transduced with shDLK-4H (Supplementary Fig. S5*A* and *B*). However, expression of *HASH-1* (*ASCL1*), a gene involved in early sympathetic lineage commitment (5), was decreased during RA-induced differentiation (Supplementary Fig. S5*A*), but not upon transduction of the lentiviral shDLK-4H (Supplementary Fig. S5*B*), suggesting nonoverlapping pathways may be involved between RA- and shDLK-induced differentiation. These results clearly show that loss of *DLK1* predisposes NB cells to spontaneous differentiation.

On the other hand, overexpression of DLK-FL significantly suppressed RA-induced neurite formation ($P < 0.0001$ versus RA-treated control; Fig. 2*C*) and resulted in increased levels of the stem cell markers CD133 and Notch1 (Fig. 2*D*), suggesting enhanced stem cell characteristics. Collectively, these data suggest a critical role of *DLK1* in the maintenance of undifferentiated NB cell phenotype.

In addition, we found that DLK1 may have an impact on other cytoplasmic pathways actively involved in neural stem cells including epidermal growth factor receptor (EGFR), fibroblast growth factor receptor (FGFR), and Notch (31–36). Levels of EGFR, FGFR1, and Notch were strongly reduced (Supplementary Fig. S6*A, C,* and *E*) in cells treated with RA or BrdUrd, as well as *DLK1* knockdown (Supplementary Fig. S6*B, D,* and *F*). On the other hand, ERK phosphorylation was strongly increased in BE(2)C cells treated by RA or BrdUrd (Supplementary Fig. S6*G*), as well as by shRNA (Supplementary Fig. S6*H*), which is consistent with increased ERK phosphorylation during differentiation of neuronal progenitor cells (37). Together, these observations show that multiple signaling pathways are potentially involved during shDLK-induced spontaneous differentiation of NB cells. However, it remains to be determined

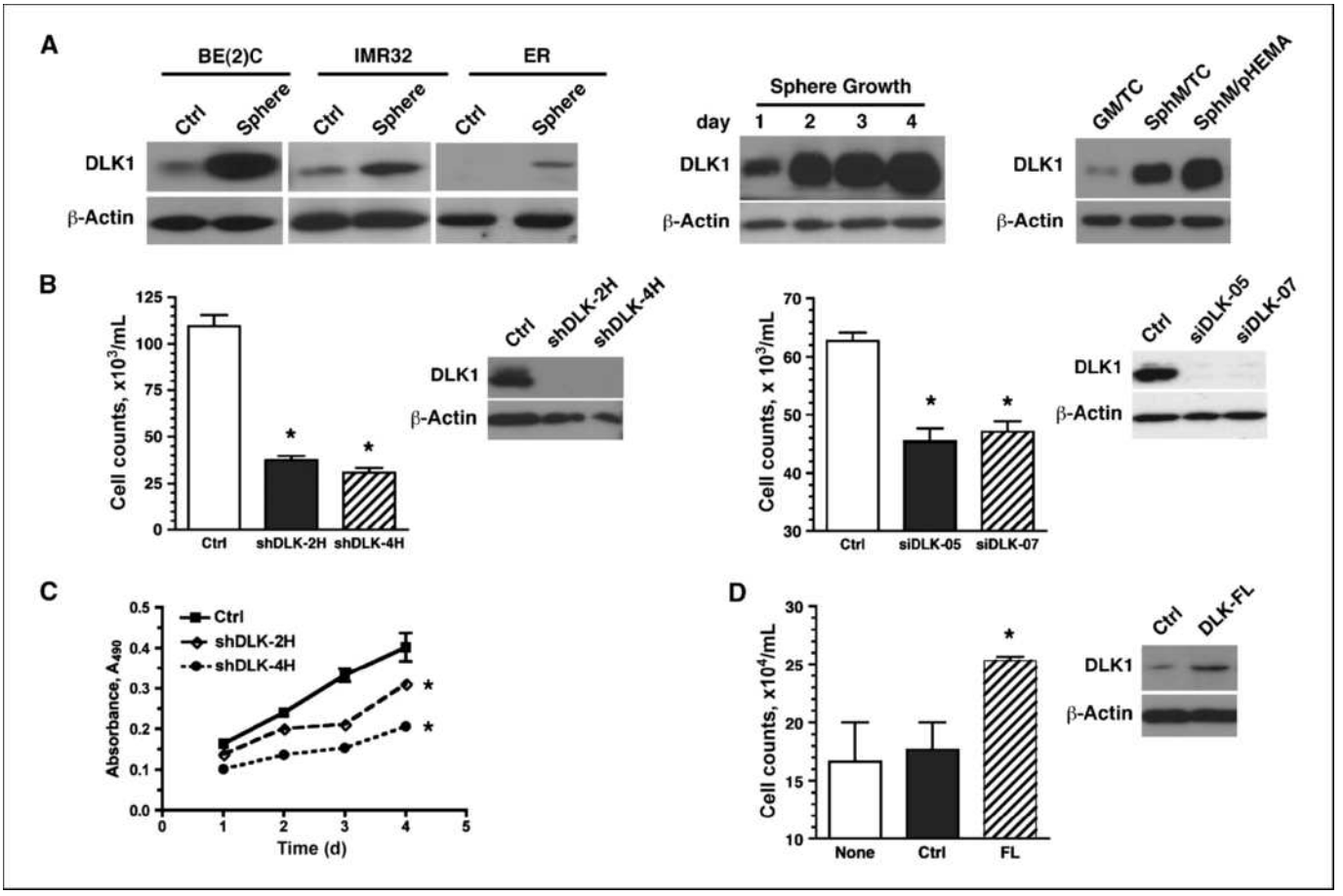

Figure 3. DLK1 regulates tumor sphere formation. *A, left,* DLK1 expression in NB cell lines cultured in sphere medium (*sphere*) or in standard growth media (*ctrl*). *Middle,* kinetics of DLK1 expression during sphere formation in BE(2) cells cultured in sphere media (*SphM*) for 1 to 4 d. *Right,* DLK1 expression in BE(2) cells cultured for 2 d in tissue culture dishes with growth medium (*GM/TC*), tissue culture dishes with sphere media (*SphM/TC*), or polyHEMA-coated dishes with sphere media (*SphM/pHEMA*). *B,* BE(2)C cells were infected with lentivirus [shDLK-2H, shDLK-4H, or vector (*ctrl*); *left*] or transfected with siRNA oligos [siDLK-05, siDLK-07, or a nontargeting siRNA (ctrl); *right*]. Cells were plated at 48 h into polyHEMA-coated six-well plates and cultured for 4 d in sphere medium. Spheres were collected and then trypsinized for cell counting (*columns,* mean; *bars,* SEM; $n = 6$; *, $P < 0.0003$ versus control). DLK1 knockdown was confirmed by Western blot. *C,* BE(2)C cells were infected with lentivirus expressing shDLK-2H, shDLK-4H, or vector (*ctrl*). Cell growth was measured daily using the MTS assay (*points,* mean; *bars,* SEM; $n = 4$; *, $P < 0.05$ versus control, one-way ANOVA). *D,* FACS-sorted SY5Y cells [DLK-FL or empty vector (*ctrl*)] and uninfected cells (*none*) were cultured in the sphere medium for 5 d. Cells in tumor spheres were counted (*columns,* mean; *bars,* SEM; $n = 6$; *, $P < 0.04$ versus control). DLK1 expression was confirmed by Western blot.

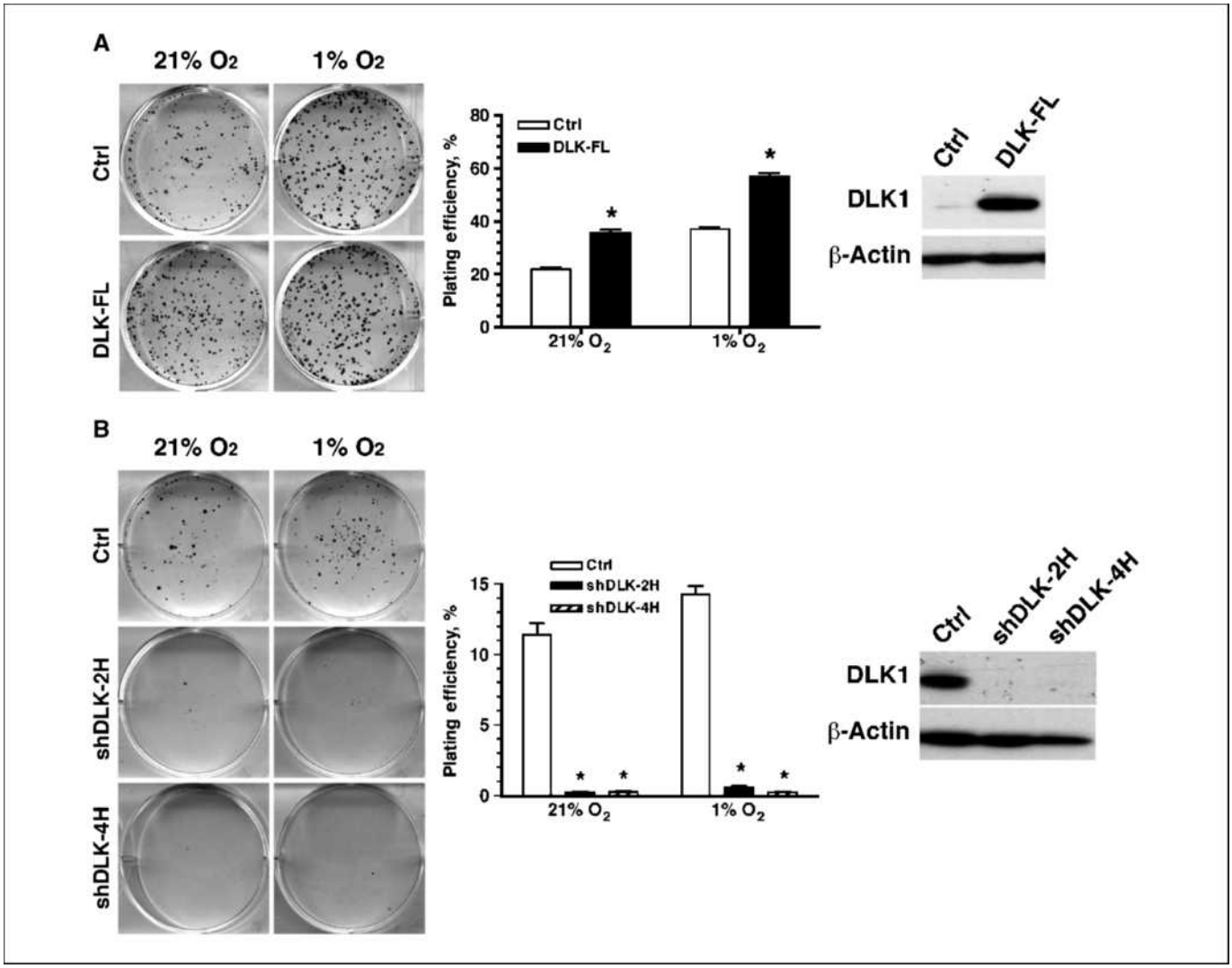

Figure 4. DLK1 regulates clonogenic growth *in vitro*. *A,* ER cells were FACS-sorted for stable expression of DLK-FL or empty vector (*ctrl*). *B,* BE(2)C cells were infected with lentivirus expression shDLK-2H, shDLK-4H, or empty vector (*ctrl*). *Left,* representative images of colonies. *Middle,* plating efficiency = % colonies per input ± SEM ($n = 6$; *, $P < 0.0001$ versus respective control). *Right,* Western blot.

whether DLK1 directly regulates these different pathways. Furthermore, it is worth noting that elevated *NPY* expression (Supplementary Fig. S5*B*) and ERK phosphorylation (Supplementary Fig. S5*C*) still occurred in shDLK-transduced cells under hypoxia, suggesting that hypoxia is not able to completely block the shDLK-induced spontaneous differentiation.

***DLK1* regulates tumor sphere formation.** The ability to grow as nonadherent spheroids in the sphere medium has been widely used to assess cancer stem cell characteristics (30, 38). All four NB cell lines used in this study were able to form tumor spheres (Supplementary Fig. S7*A*), albeit to different degrees. DLK1 expression was strongly increased in tumor spheres compared with adherent cells maintained in the serum-containing medium (Fig. 3*A, left*). When plated in tissue culture dishes, BE(2)C cells formed tumor spheres gradually in the sphere medium (Supplementary Fig. S7*B*). Interestingly, DLK1 expression increased as the tumor spheres grew (Fig. 3*A, middle*), further suggesting a relationship between enhanced DLK1 expression and tumor sphere formation.

To ascertain that increased *DLK1* expression results from sphere formation and not just the effects of the sphere medium, we compared DLK1 expression under three different conditions: (*a*) as a monolayer in tissue culture dishes with the regular growth medium (*GM/TC*), (*b*) as a mixture of adherent and nonadherent cells in tissue culture dishes with the sphere medium (*SphM/TC*), or (*c*) as completely nonadherent culture in polyHEMA-coated dishes with the sphere medium (*SphM/pHEMA*). As shown in Fig. 3*A* (*right*), the sphere medium generally enhanced DLK1 expression over the GM/TC control. More robust increases of DLK1 expression occurred under the SphM/pHEMA condition that forced formation of tumor spheres. We further determined whether hypoxia developed in the growing tumor spheres using the hypoxia marker pimonidazole hydrochloride (hypoxyprobe-1). Only ≤16% cells became hypoxic in the 6-day-old tumor spheres (Supplementary Fig. S7*C*), suggesting that the increased DLK1 expression in tumor spheres is unlikely to be driven by hypoxia. Because the "sphere culture" condition facilitates the expansion or enrichment of stem cells and/or progenitors, NB cells growing as spheroids likely possess enhanced stem

cell characteristics. Therefore, increased DLK1 expression under the "sphere culture" condition may be associated with enhanced stem cell characteristics.

BE(2)C cells were only able to form loose cell aggregates (Supplementary Fig. S7*A*), which made it difficult to accurately measure the sizes or the numbers of spheres/aggregates. Therefore, we examined the role of *DLK1* in regulating tumor sphere growth by enumerating total cell numbers in tumor spheres. We found that knocking down *DLK1* expression with the shRNA constructs (Fig. 3*B, left*) or the siRNA oligonucleotides (Fig. 3*B, right*) resulted in a significant decrease in tumor sphere growth. The shDLK constructs also decreased cell growth when cells were maintained in the regular medium (Fig. 3*C*), consistent with its role in facilitating spontaneous differentiation. Conversely, expression of DLK-FL in SY5Y cells (DLK1-low) enhanced tumor sphere growth (Fig. 3*D*). However, overexpression of DLK-FL did not change the growth rate of SY5Y cells under the conventional culture condition (Supplementary Fig. S7*D*). Nonetheless, these results show that *DLK1* plays an important role in regulating the ability of NB cells to grow as anchorage-independent tumor spheres, an important aspect of cancer stem cell characteristics.

***DLK1* promotes clonogenicity *in vitro*.** Clonogenicity measures the ability to form a colony from a single cell or the self-renewal potential. As shown in Fig. 4*A*, overexpression of DLK-FL in ER cells (DLK-low) significantly enhanced clonogenicity (% plating efficiency) under both normoxia and hypoxia, whereas shRNA-mediated knockdown of endogenous *DLK1* in BE(2)C cells (DLK1-high) resulted in a dramatic decrease of clonogenicity (Fig. 4*B*). Similarly, transient transfection with the siRNA oligonucleotides also significantly decreased clonogenic growth of BE(2)C cells (Supplementary Fig. S8), albeit less potently than the lentiviral shRNAs. This difference is likely due to the short-term effects of oligonucleotides compared with the constitutively expressed shRNAs.

The DLK1 intracellular domain (~50 amino acids) contains two putative phosphorylation sites Y339 and S355 that are highly conserved among mammals (Fig. 5*A*), suggesting that the DLK1 cytoplasmic domain may be required for its biological functions. To test this hypothesis, we created the following retroviral constructs:

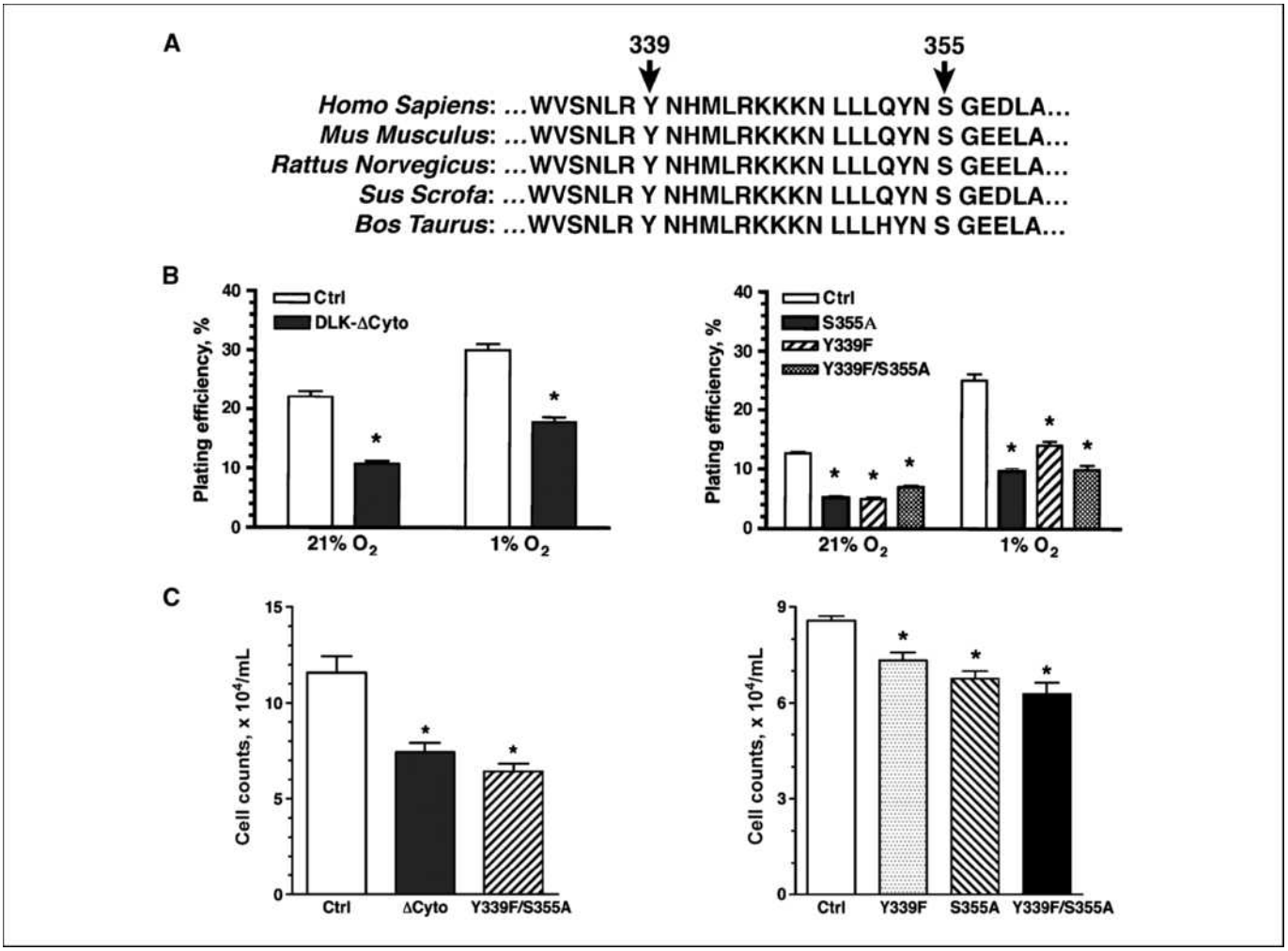

Figure 5. DLK1 cytoplasmic domain is required for clonogenic growth and tumor sphere formation. *A,* comparison of the DLK1 cytoplasmic domains among different mammalian species. *Arrows,* the putative phosphorylation sites [tyrosine (Y)-339 and serine (S)-355]. *B,* BE(2)C cells were FACS-sorted for DLK1 lacking cytoplasmic domain (*DLK-ΔCyto*; *left*), DLK1 with point mutation [Y339F (phenylalanine), S355A (alanine), or Y339F/S355A; *right*] or empty vector (*ctrl*). Clonogenic assays were performed as described in Fig. 4. *, $P < 0.0002$ versus control. *C,* FACS-sorted BE(2)C cells were cultured in the sphere medium for 4 d (Fig. 3*B*). *, $P < 0.002$ versus control.

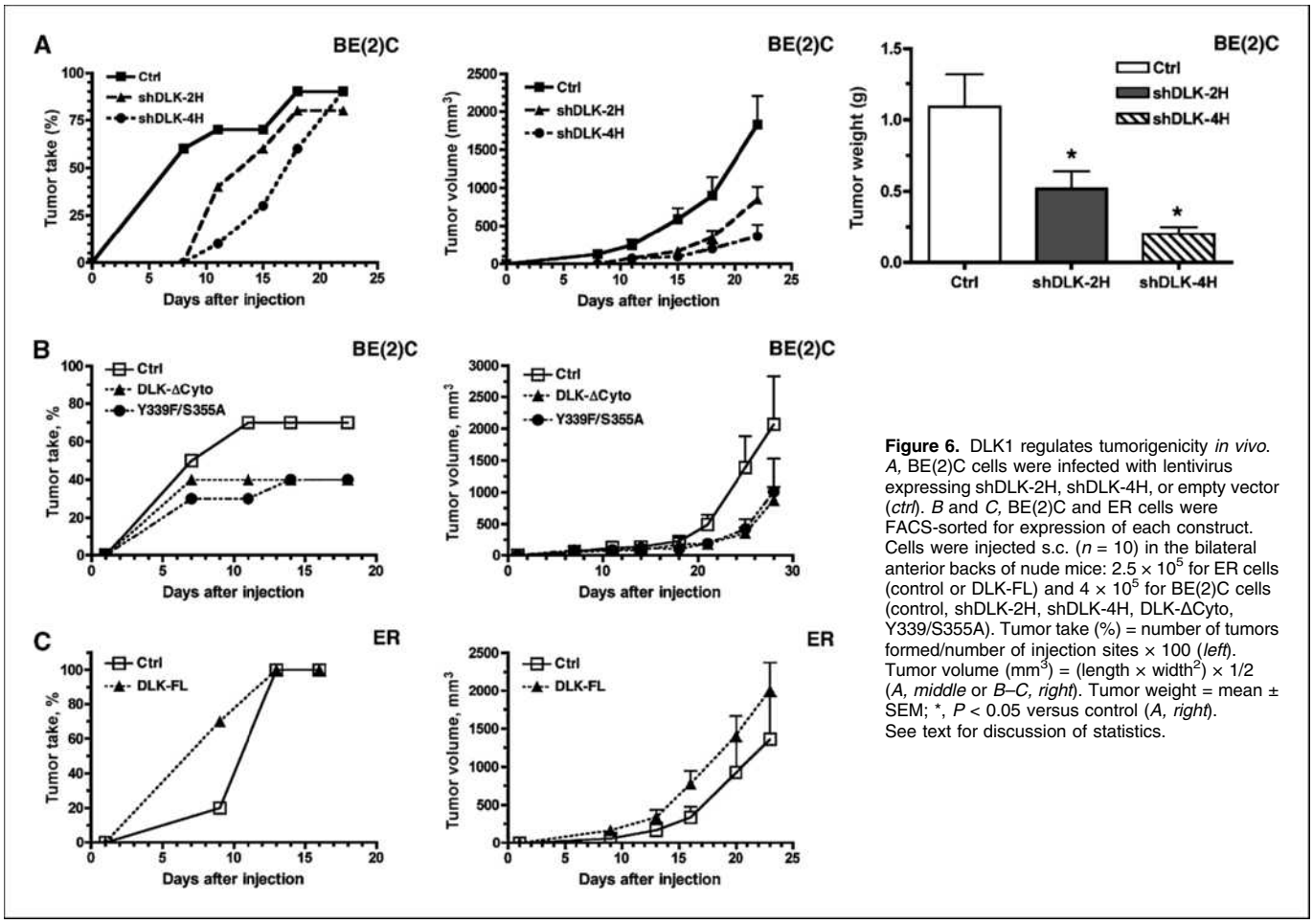

Figure 6. DLK1 regulates tumorigenicity *in vivo*. *A,* BE(2)C cells were infected with lentivirus expressing shDLK-2H, shDLK-4H, or empty vector (*ctrl*). *B* and *C,* BE(2)C and ER cells were FACS-sorted for expression of each construct. Cells were injected s.c. ($n = 10$) in the bilateral anterior backs of nude mice: 2.5×10^5 for ER cells (control or DLK-FL) and 4×10^5 for BE(2)C cells (control, shDLK-2H, shDLK-4H, DLK-ΔCyto, Y339/S355A). Tumor take (%) = number of tumors formed/number of injection sites × 100 (*left*). Tumor volume (mm^3) = (length × $width^2$) × 1/2 (*A, middle* or *B–C, right*). Tumor weight = mean ± SEM; *, $P < 0.05$ versus control (*A, right*). See text for discussion of statistics.

(*a*) DLK1 cytoplasmic domain deletion (DLK-ΔCyto), (*b*) full-length DLK1 with a single mutation, Y339-to-phenylalanine(F) or S355-to-alanine(A), and (*c*) full-length DLK1 with both mutations (Y339F/S355A). BE(2)C cells with stable expression of DLK-ΔCyto, Y339F, S355A, or Y339F/S355A exhibited significantly reduced clonogenicity under both normoxia and hypoxia (Fig. 5*B*), as well as decreased growth of tumor spheres (Fig. 5*C*). These results suggest that the DLK1 cytoplasmic domain may play an essential role in facilitating clonogenic growth and tumor sphere formation. However, DLK-ΔCyto and Y339F/S355A did not appear to have significant impact on either spontaneous differentiation or cell growth under conventional tissue culture conditions. It is likely that the two DLK1 mutants exert their dominant-negative effects only under certain stress conditions, such as in the tumor sphere media or under the clonogenic conditions.

***DLK1* promotes tumorigenicity *in vivo*.** Using the subcutaneous xenograft assay in athymic mice, we found that BE(2)C cells with shRNA-mediated downregulation of *DLK1* expression exhibited longer tumor delay (Fig. 6*A, left*). Both shDLK-2H and shDLK-4H tumors were significantly smaller in volume during growth ($P < 0.002$ for each group versus control; Fig. 6*A, middle*) and by weight at the end of the experiment ($P < 0.05$ for each group versus control; Fig. 6*A, right*). Interestingly, overexpression of both DLK-ΔCyto and Y339F/S355A mutants in BE(2)C cells decreased overall tumor take rate and retarded tumor growth (Fig. 6*B*). Statistically, the Y339F/S355A tumors were smaller ($P = 0.044$) and grew more slowly ($P = 0.022$) than the vector control within the first 21 days of growth. Tumor growth rate appeared to be similar during the late stage of tumor growth. The mean growth rate of the DLK-ΔCyto tumors was nearly identical to that of the Y339F/S355A tumors. However, the differences between the DLK-ΔCyto and the control group were not statistically significant, likely due to the variability among individual tumor sizes. Nonetheless, these data suggest that the DLK-ΔCyto and Y339F/S355A mutants may possess dominant-negative functions.

On the other hand, overexpression of DLK-FL in ER cells (DLK1-low) accelerated tumor take or shortened tumor latency (Fig. 6*C*). Tumors developed from ER cells with DLK-FL were larger ($P < 0.01$) and grew faster ($P < 0.04$) than the control cells (Fig. 6*C*). However, the difference in the growth rate between the DLK-FL and the control group appears to narrow after day 16. Nevertheless, results from our additional xenograft experiments also showed that DLK-FL enhanced tumorigenicity, whereas DLK-ΔCyto and Y339F/S355A decreased tumorigenicity (Supplementary Fig. S9). These results indicate that DLK1 plays an important role in the regulation of tumorigenicity *in vivo*.

Discussion

Hypoxia is an important environmental factor that seems to favor undifferentiated stem or progenitor cells, including human embryonic stem cells, neuronal, and other mesenchymal progenitor cells (9, 10, 12, 20). Jögi and colleagues (5) have shown that hypoxic NB cells acquire an immature phenotype and that hypoxia-pretreated

NB cells grow slightly faster *in vivo*. Recent genomics studies have further revealed that poorly differentiated human tumors display a gene expression signature similar to that found in normal embryonic stem cells (39) or lineage-committed progenitor cells (40). However, it remains largely unknown how stem cell genes regulate tumor progression, and how their expression is regulated by tumor microenvironment.

DLK1, a member of the *notch/delta/serrate* family, is preferentially expressed in immature cells with regenerative potentials (13, 15). *DLK1* inhibits adipogenesis (24) and also seems to regulate the differentiation of hematopoietic stem cells (17, 19) and lymphoid progenitors (41, 42). Elevated expression of *DLK1* is found in a variety of tumor cells, including NB (18), gliomas (16), small-cell lung carcinoma (43), and leukemia (17, 19). Other evidence suggests that *DLK1* may inhibit tumor cell differentiation and increase proliferation (16, 19). Nonetheless, the role of *DLK1* in tumor progression remains poorly understood.

In this report, we have shown that hypoxia increases *DLK1* expression via the HIF-dependent mechanism. *DLK1* knockdown results in enhanced spontaneous differentiation of NB cells, reduced tumor sphere growth, decreased clonogenicity *in vitro*, and decreased tumorigenicity *in vivo*. On the other hand, overexpression of *DLK1* inhibits differentiation and promotes tumorigenicity. Our data have further revealed an important role of the DLK1 cytoplasmic domain, especially the conserved putative phosphorylation sites Y339 and S355. Consistent with our findings, Li and colleagues (19) have found that the DLK1 cytoplasmic domain is required for blocking RA-induced differentiation of human promyelocytic HL-60 cells. Our observations have provided strong evidence establishing *DLK1* as a new class of stem cell genes that play a significant role in the regulation of cancer stem cell characteristics and tumorigenicity.

Our data suggest that DLK1 can exert potential impact on several membrane-associated signaling pathways including EGFR, FGFR, and Notch that facilitate maintenance or self-renewal of neural stem/progenitor cells (31–36), as well as ERK phosphorylation (37). Obviously, the mechanisms of DLK1 function likely involve multiple pathways. We cannot rule out the possibility that changes in these signaling pathways result from shDLK-induced spontaneous differentiation, rather than directly from the loss of interaction with DLK1. The exact mechanisms of DLK1 function warrant further investigation.

Recent studies have shown that a small population of immature NB tumor cells is localized in a perivascular space *in vivo* and shows strong immunochemical staining for HIF-2α (7, 44). These HIF-2α$^+$ cells also seem to be positive for *MYCN* amplification (44). However, we have found that HIF-2α is differentially expressed in NB cell lines, although HIF-1α is ubiquitously expressed and does not correlate with *MYCN* amplification. It is possible that HIF-1α and HIF-2α are regulated by different mechanisms, especially under *in vivo* conditions. Consistent with this notion, our previous study (11) has found that HIF-2α is expressed only in the differentiated adipocytes, but not in the progenitor cells, and is stabilized at 21% O_2. It seems that elevated HIF-2α expression is preferentially associated with a stem cell–like population from NB tumors (7, 44) or gliomas (8). Since our data have shown that both HIF-1α and HIF-2α are capable of enhancing *DLK1* transcription, it will be of great interest to determine whether elevated HIF-2α expression, especially in such perivascular niches, has an effect on *DLK1* expression *in vivo*. Our observations, together with others, support a new paradigm that hypoxia signaling promotes tumor progression by upregulation of stem cell genes including *DLK1* that facilitate the maintenance or selection of cancer cells with stem cell characteristics.

Disclosure of Potential Conflicts of Interest

No potential conflicts of interest were disclosed.

Acknowledgments

Received 4/30/09; revised 9/10/09; accepted 10/6/09; published OnlineFirst 11/24/09.

Grant support: NIH grant R01CA125021 (Z. Yun). Y. Kim is supported in part by an institutional postdoctoral training grant (5-T32-CA009259) from the NIH and the Anna Fuller Fund Fellowship from Yale University School of Medicine.

The costs of publication of this article were defrayed in part by the payment of page charges. This article must therefore be hereby marked *advertisement* in accordance with 18 U.S.C. Section 1734 solely to indicate this fact.

We thank Dr. Nai-Kong V. Cheung of Memorial Sloan-Kettering Cancer Center for SK-N-ER cells, Dr. Robert Ross of Fordham University for BE(2)C cells, Dr. A.N. Van den Pol of Yale University for the human astrocytic progenitors from adult brain and embryonic tissues, Dr. Ravi Bhatia of City of Hope National Medical Center for full-length DLK1 and DLK1-ΔCyto, Dr. Frank Lee of the University of Pennsylvania for HIF-2αP531A, Dr. Kazufumi Katayama of the Tokyo Metropolitan Institute of Medical Science for the lentiviral shRNA vectors, members of the Yun Laboratory, especially Dr. Yongming Ren, for constructive suggestions and technical assistance, and Lisa Cabral for her excellent editorial assistance.

References

1. Clarke MF, Dick JE, Dirks PB, et al. Cancer stem cells-perspectives on current status and future directions: AACR Workshop on cancer stem cells. Cancer Res 2006;66:9339–44.
2. Adams JM, Strasser A. Is tumor growth sustained by rare cancer stem cells or dominant clones? Cancer Res 2008;68:4018–21.
3. Vaupel P, Mayer A. Hypoxia in cancer: significance and impact on clinical outcome. Cancer Metastasis Rev 2007;26:225–39.
4. Das B, Tsuchida R, Malkin D, Koren G, Baruchel S, Yeger H. Hypoxia enhances tumor stemness by increasing the invasive and tumorigenic side population fraction. Stem Cells 2008;26:1818–30.
5. Jogi A, Ora I, Nilsson H, et al. Hypoxia alters gene expression in human neuroblastoma cells toward an immature and neural crest-like phenotype. Proc Natl Acad Sci U S A 2002;99:7021–6.
6. Couvelard A, O'Toole D, Turley H, et al. Microvascular density and hypoxia-inducible factor pathway in pancreatic endocrine tumours: negative correlation of microvascular density and VEGF expression with tumour progression. Br J Cancer 2005;92:94–101.
7. Holmquist-Mengelbier L, Fredlund E, Lofstedt T, et al. Recruitment of HIF-1α and HIF-2α to common target genes is differentially regulated in neuroblastoma: HIF-2α promotes an aggressive phenotype. Cancer Cell 2006;10:413–23.
8. Li Z, Bao S, Wu Q, et al. Hypoxia-inducible factors regulate tumorigenic capacity of glioma stem cells. Cancer Cell 2009;15:501–13.
9. Ezashi T, Das P, Roberts RM. Low O2 tensions and the prevention of differentiation of hES cells. Proc Natl Acad Sci U S A 2005;102:4783–8.
10. Gustafsson MV, Zheng X, Pereira T, et al. Hypoxia requires notch signaling to maintain the undifferentiated cell state. Dev Cell 2005;9:617–28.
11. Lin Q, Lee YJ, Yun Z. Differentiation arrest by hypoxia. J Biol Chem 2006;281:30678–83.
12. Yun Z, Maecker HL, Johnson RS, Giaccia AJ. Inhibition of PPARg2 gene expression by the HIF-1-regulated gene DEC1/Stra13: a mechanism for regulation of adipogenesis by hypoxia. Dev Cell 2002;2:331–41.
13. Floridon C, Jensen CH, Thorsen P, et al. Does fetal antigen 1 (FA1) identify cells with regenerative, endocrine and neuroendocrine potentials? A study of FA1 in embryonic, fetal, and placental tissue and in maternal circulation. Differentiation 2000;66:49–59.
14. Jensen CH, Krogh TN, Hojrup P, et al. Protein structure of fetal antigen 1 (FA1). A novel circulating human epidermal-growth-factor-like protein expressed in neuroendocrine tumors and its relation to the gene products of dlk and pG2. Eur J Biochem 1994;225:83–92.
15. Tornehave D, Jensen CH, Teisner B, Larsson LI. FA1 immunoreactivity in endocrine tumours and during development of the human fetal pancreas; negative correlation with glucagon expression. Histochem Cell Biol 1996;106:535–42.
16. Yin D, Xie D, Sakajiri S, et al. DLK1: increased expression in gliomas and associated with oncogenic activities. Oncogene 2006;25:1852–61.
17. Sakajiri S, O'Kelly J, Yin D, et al. Dlk1 in normal and abnormal hematopoiesis. Leukemia 2005;19:1404–10.

18. Van Limpt VA, Chan AJ, Van Sluis PG, Caron HN, Van Noesel CJ, Versteeg R. High δ-like 1 expression in a subset of neuroblastoma cell lines corresponds to a differentiated chromaffin cell type. Int J Cancer 2003;105:61–9.
19. Li L, Forman SJ, Bhatia R. Expression of DLK1 in hematopoietic cells results in inhibition of differentiation and proliferation. Oncogene 2005;24:4472–6.
20. Yun Z, Lin Q, Giaccia AJ. Adaptive myogenesis under hypoxia. Mol Cell Biol 2005;25:3040–55.
21. Percy MJ, Furlow PW, Lucas GS, et al. A gain-of-function mutation in the HIF2A gene in familial erythrocytosis. N Engl J Med 2008;358:162–8.
22. Katayama K, Wada K, Miyoshi H, et al. RNA interfering approach for clarifying the PPARγ pathway using lentiviral vector expressing short hairpin RNA. FEBS Lett 2004;560:178–82.
23. Hirama M, Takahashi F, Takahashi K, et al. Osteopontin overproduced by tumor cells acts as a potent angiogenic factor contributing to tumor growth. Cancer Lett 2003;198: 107–17.
24. Villena JA, Kim KH, Sul HS. Pref-1 and ADSF/resistin: two secreted factors inhibiting adipose tissue development. Horm Metab Res 2002;34:664–70.
25. Wenger RH, Stiehl DP, Camenisch G. Integration of oxygen signaling at the consensus HRE. Sci STKE 2005; 2005:re12.
26. Bindra RS, Glazer PM. Repression of RAD51 gene expression by E2F4/p130 complexes in hypoxia. Oncogene 2007;26:2048–57.
27. Hu CJ, Iyer S, Sataur A, Covello KL, Chodosh LA, Simon MC. Differential regulation of the transcriptional activities of hypoxia-inducible factor 1 α (HIF-1α) and HIF-2α in stem cells. Mol Cell Biol 2006;26:3514–26.
28. Ross RA, Biedler JL, Spengler BA. A role for distinct cell types in determining malignancy in human neuroblastoma cell lines and tumors. Cancer Lett 2003;197:35–9.
29. Walton JD, Kattan DR, Thomas SK, et al. Characteristics of stem cells from human neuroblastoma cell lines and in tumors. Neoplasia 2004;6:838–45.
30. Hemmati HD, Nakano I, Lazareff JA, et al. Cancerous stem cells can arise from pediatric brain tumors. Proc Natl Acad Sci U S A 2003;100:15178–83.
31. Bachoo RM, Maher EA, Ligon KL, et al. Epidermal growth factor receptor and Ink4a/Arf: convergent mechanisms governing terminal differentiation and transformation along the neural stem cell to astrocyte axis. Cancer Cell 2002;1:269–77.
32. Boockvar JA, Kapitonov D, Kapoor G, et al. Constitutive EGFR signaling confers a motile phenotype to neural stem cells. Mol Cell Neurosci 2003;24:1116–30.
33. Ivkovic S, Canoll P, Goldman JE. Constitutive EGFR signaling in oligodendrocyte progenitors leads to diffuse hyperplasia in postnatal white matter. J Neurosci 2008; 28:914–22.
34. Maric D, Fiorio Pla A, Chang YH, Barker JL. Self-renewing and differentiating properties of cortical neural stem cells are selectively regulated by basic fibroblast growth factor (FGF) signaling via specific FGF receptors. J Neurosci 2007;27:1836–52.
35. Saarimaki-Vire J, Peltopuro P, Lahti L, et al. Fibroblast growth factor receptors cooperate to regulate neural progenitor properties in the developing midbrain and hindbrain. J Neurosci 2007;27:8581–92.
36. Pahlman S, Stockhausen MT, Fredlund E, Axelson H. Notch signaling in neuroblastoma. Semin Cancer Biol 2004;14:365–73.
37. Berwick DC, Calissano M, Corness JD, Cook SJ, Latchman DS. Regulation of Brn-3a N-terminal transcriptional activity by MEK1/2-ERK1/2 signalling in neural differentiation. Brain Res 2009;1256:8–18.
38. Hansford LM, McKee AE, Zhang L, et al. Neuroblastoma cells isolated from bone marrow metastases contain a naturally enriched tumor-initiating cell. Cancer Res 2007;67:11234–43.
39. Ben-Porath I, Thomson MW, Carey VJ, et al. An embryonic stem cell-like gene expression signature in poorly differentiated aggressive human tumors. Nat Genet 2008;40:499–507.
40. Phillips HS, Kharbanda S, Chen R, et al. Molecular subclasses of high-grade glioma predict prognosis, delineate a pattern of disease progression, and resemble stages in neurogenesis. Cancer Cell 2006;9: 157–73.
41. Bauer SR, Ruiz-Hidalgo MJ, Rudikoff EK, Goldstein J, Laborda J. Modulated expression of the epidermal growth factor-like homeotic protein dlk influences stromal-cell-pre-B-cell interactions, stromal cell adipogenesis, and pre-B-cell interleukin-7 requirements. Mol Cell Biol 1998;18:5247–55.
42. Kaneta M, Osawa M, Sudo K, Nakauchi H, Farr AG, Takahama Y. A role for pref-1 and HES-1 in thymocyte development. J Immunol 2000;164:256–64.
43. Laborda J, Sausville EA, Hoffman T, Notario V. dlk, a putative mammalian homeotic gene differentially expressed in small cell lung carcinoma and neuroendocrine tumor cell line. J Biol Chem 1993;268:3817–20.
44. Pietras A, Gisselsson D, Ora I, et al. High levels of HIF-2α highlight an immature neural crest-like neuroblastoma cell cohort located in a perivascular niche. J Pathol 2008;214:482–8.